Optimization of Envelope Tracking Power Amplifier for Base-Station Applications

Jungjoon Kim, *Student Member, IEEE*, Jungwhan Son, *Student Member, IEEE*, Seunghoon Jee, Seokhyeon Kim, and Bumman Kim, *Fellow, IEEE*

***Abstract*—We have proposed two methods of enhancing efficiency of an envelope tracking power amplifier (ET PA) from an interlock operation. The first is the utilization of sinking current. The sinking current is a critical efficiency reduction factor since it is a wasted power. To reduce the sinking current, the gate bias of the power amplifier (PA) is increased so that the sinking current is delivered to the PA and is utilized for amplification. The other one is the RF input shaping method. The input signal of ET PAs is a modulated RF signal, and the signal does not guarantee fully saturated operation of the PA at all power levels due to g_m nonlinearity of a device. To obtain the maximum efficiency for all of the envelope voltage, we have found the optimum RF input conditions and applied it to the input of the PA. To verify the methods, the proposed ET PA is implemented using a Cree CGH40045 GaN HEMT. For a long-term evolution 5-MHz signal with 6.5-dB peak-to-average power ratio, the PA delivers power-added efficiency of 58.76% with 40.14-dBm output power at 889 MHz.**

***Index Terms*—Efficiency, envelope shaping, envelope tracking (ET), ET power amplifier (ET PA), peak-to-average ratio, power amplifier (PA).**

I. Introduction

FOR RECENT communication systems, a highly efficient power amplifier (PA) is essential because the high efficiency guarantees improved thermal management, lower cost, and good reliability [1]–[4]. The conventional class-AB amplifier is no longer attractive for a high peak-to-average power ratio (PAPR) signal due to its poor efficiency at a backed-off region, and a number of efficiency enhancement techniques have been studied [5]–[14]. Among them, the envelope tracking (ET) technique has received a lot of attention recently [11]–[14].

Since the dc supply power of the ET PA is dynamically adjusted to the proper level, the PA is operated at a high efficiency for all power levels. In case of a standalone PA [see Fig. 1(a)], the difference between the fixed supply voltage and the transmitted envelope voltage is dissipated as heat, reducing the efficiency. However, for an ET PA [see Fig. 1(b)], the modulated supply voltage accurately tracks the transmitted signal, and has a high efficiency for all power level. For a proper operation of the ET PA, however, a highly efficient supply modulator with a good linearity is essential.

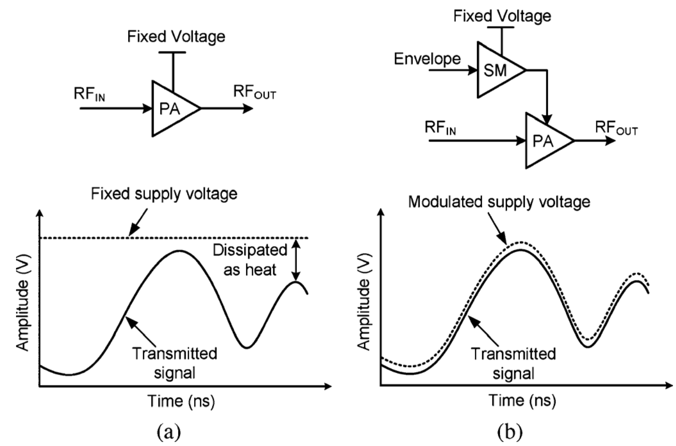

Fig. 1. Concept of: (a) standalone PA and (b) ET PA.

The most popular supply modulator is a hybrid switching amplifier (HSA) [15], [16], which is shown in Fig. 2. The HSA consists of a linear stage as an accurate voltage source and a switching stage as a dependent current source, and it supplies the envelope signal linearly with high efficiency.

The switching stage cannot follow the signal speed, and operates as a quasi-constant current source. The error in generating the envelope signal is compensated by the linear amplifier, by generating a sourcing current and a sinking current. Many methods have been studied to improve the efficiency of the ET PAs, such as improving the structure of the supply modulator and designing the highly efficient PA separately [13]–[20]. Since the ET PA is based on the interlocking operation between the supply modulator and the PA, the two parts should be considered as an integrated one for optimized operation of the ET PA.

In this paper, we have focused on the interlock operation between the supply modulator and the PA to enhance the efficiency of the ET PA. In Section II, various envelope shaping methods are introduced and we have proposed a new current shaping method. In Section III, we have searched for the optimum RF input shaping (RFIS) method to achieve a maximum efficiency of the PA for all power level. To verify the proposed methods (Sections II and III), the optimized ET PA is implemented at 889 MHz using a GaN HEMT device, and the results are shown in Section IV.

Manuscript received August 24, 2012; accepted December 10, 2012. Date of publication March 11, 2013; date of current version April 02, 2013. This work was supported by the Ministry of Knowledge Economy (MKE), Korea, under the Information Technology Research Center (ITRC) Support Program supervised by the National IT Industry Promotion Agency (NIPA) [NIPA-2010-(C1090-1011-0011)], by the Ministry of Education, Science and Technology through the National Research Foundation of Korea under the World Class University Program (R31-10100), and by Brain Korea 21.

The authors are with the Department of Electrical Engineering, Division of Information Technology Convergence Engineering, Pohang University of Science and Technology, Pohang, Gyeongbuk 790-784, Korea (e-mail: jungjoon@postech.ac.kr; jhson@postech.ac.kr; cshcomit@postech.ac.kr; necmen@postech.ac.kr; bmkim@postech.ac.kr).

Digital Object Identifier 10.1109/TMTT.2013.2248375

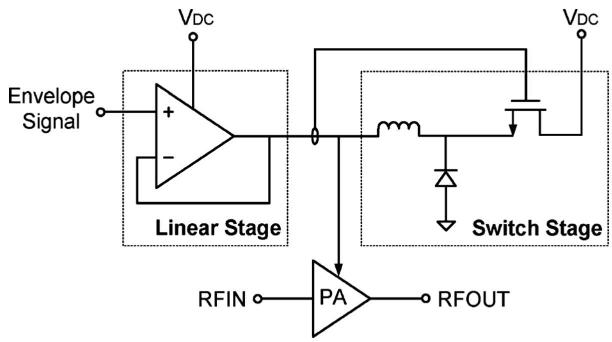

Fig. 2. Simplified circuit diagram of HSA.

II. Envelope Shaping for Improved Efficiency

The envelope signal is the only one connecting the supply modulator and the PA. Since the envelope signal is the output waveform of the supply modulator and is also the drain bias of the PA, the envelope shaping affects the characteristics of the supply modulator and the PA, and their relation is described in this section.

A long-term evolution (LTE) envelope signal is used with bandwidth (BW) of 5 MHz and PAPR of 6.5 dB for the simulation, and various envelope shapings are shown in Fig. 3, which can be expressed as follows by (1):

$$\begin{aligned} \text{Shape 1}: V_{\text{env.out}} &= 30 \cdot V_{\text{norm.in}}^{N} \\ \text{Shape 2}: V_{\text{env.out}} &= (30 - V_k) \cdot V_{\text{norm.in}} + V_k \\ \text{Shape 3}: V_{\text{env.out}} &= (30 - V_k) \cdot V_{\text{norm.in}}^{N} + V_k. \end{aligned} \tag{1}$$

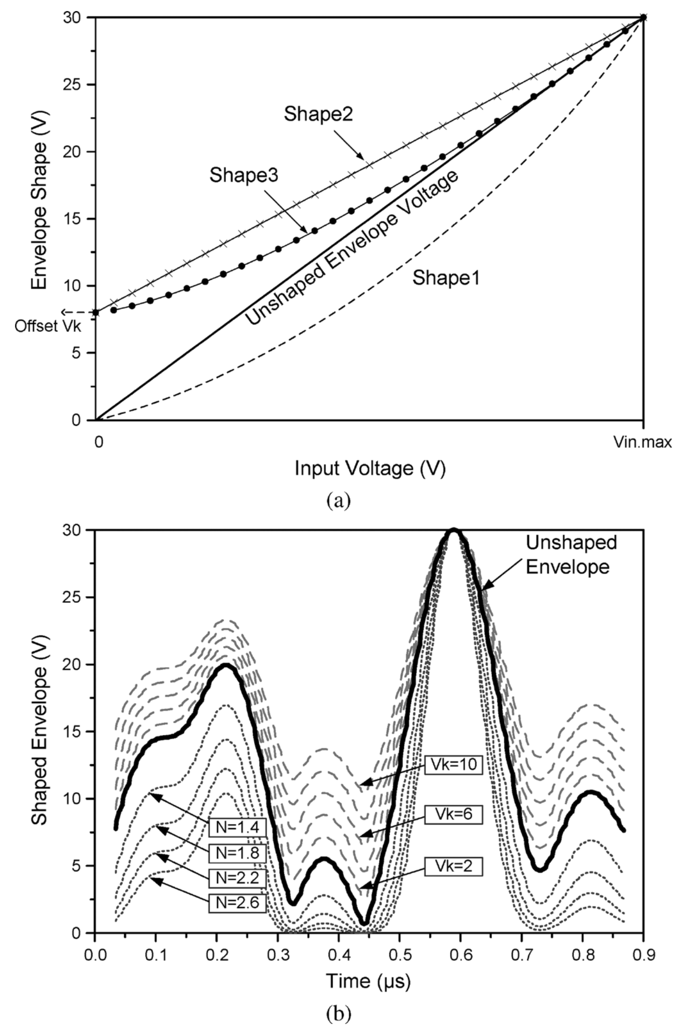

Fig. 3. (a) Various envelope shaping methods. (b) Shape in time domain.

It is assumed that the maximum drain bias is 30 V for the peak output power, the minimum envelope voltage is V_K, N denotes the curve shaping factor, and the efficiency of the supply modulator is 70% for the unshaped envelope. The characteristics of the supply modulator is changed by various envelope shaping, as shown in Fig. 4. For constant resistive load conditions [see Fig. 4(a)] [17], increasing the minimum envelope voltage makes the PAPR decrease, and the efficiency of the supply modulator increases. On the contrary, increasing N makes the PAPR increase, thus the efficiency of the PA decreases. For an ET PA, the load is not a constant resistance, but the PA itself. In this real case, the voltage is shaped, but the PA draws a current related to the RF input power, which is not shaped. For more accurate analysis, the envelope simulation is carried out for the PA load conditions and is depicted in Fig. 4(b). In this condition, the efficiency of the supply modulator is almost constant for the various V_K, but there is a small change for the value of N, the highest efficiency with $N = 1$. Therefore, the envelope voltage shaping is not effective for the efficiency enhancement.

However, the envelope current shaping can be effective for efficiency improvement of the supply modulator. In the HSA, the switching stage operates as a quasi-constant current source with high efficiency. In case of a class-B biased PA, the typical supplied current profiles are shown in Fig. 5. Among them, the oversupplied switch current is not utilized anywhere, but goes to the ground and is wasted. Therefore, the sinking current becomes a efficiency reduction factor, and should be properly utilized to enhance the overall efficiency through the current shaping, which we called utilization of the sinking current (USC) [21].

The HSA is an ideal voltage source injecting envelope voltage to the drain of the PA with supplying the current required by the PA. The PA in the ET PA is usually biased at deep class AB and the drain current is almost proportional to the envelope of the RF input signal, but not dependent on the envelope of the supply voltage. If the gate bias of the PA is changed from the deep class AB to light class AB, the quiescent bias current increases proportionally and the minimum load current of the HSA also increases. Therefore, the sinking current is not dissipated, but flows to the PA. Fig. 6 shows the load currents and switch currents versus the minimum load current. When the minimum bias current is changed from 0.6 to 1.2 A, most of the switch current flows to the load with little wasted sinking current. Although the peak-to-average ratio of the voltage remains the same, the peak-to-average ratio of the load current decreases and efficiency of the HSA rapidly increases, as shown in Fig. 7. Assuming that the switch current is 1 A and the efficiency of the switch is 90%, the calculated efficiency

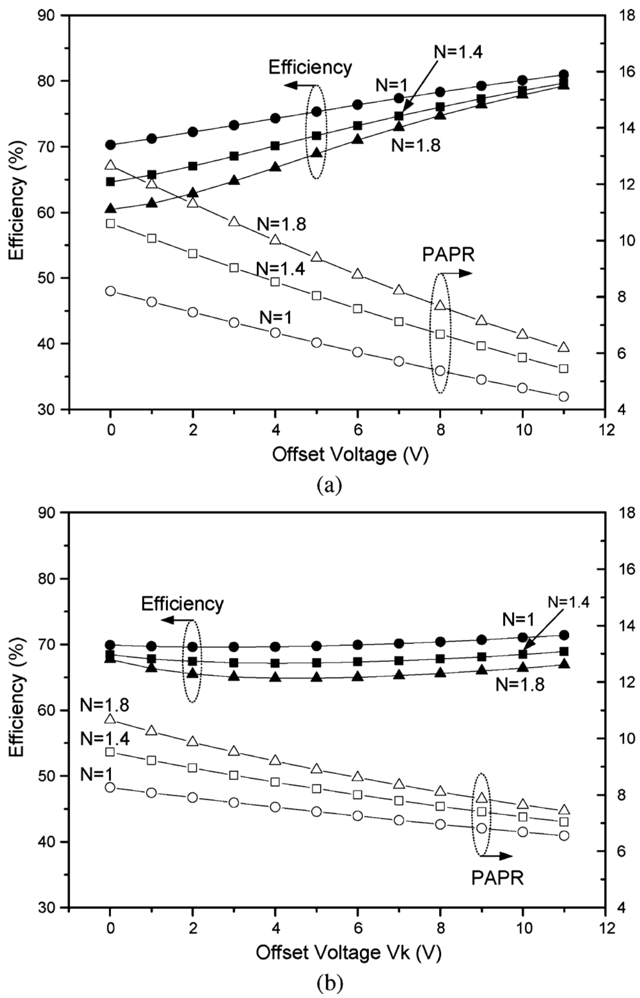

Fig. 4. Efficiency characteristic for various envelope shaping. (a) Constant load condition. (b) PA load condition.

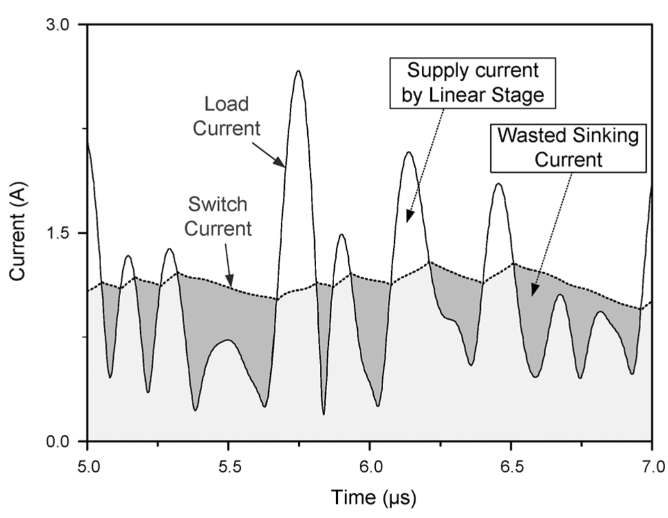

Fig. 5. Simulated output current waveforms of HSA.

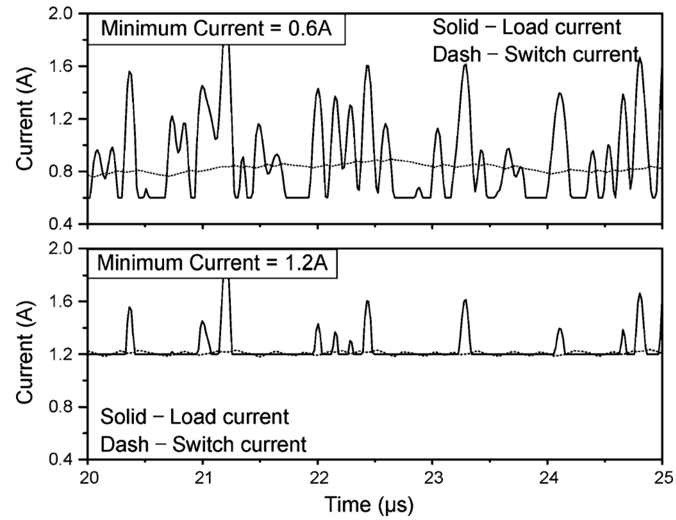

Fig. 6. Simulated output current waveforms for different minimum load current conditions.

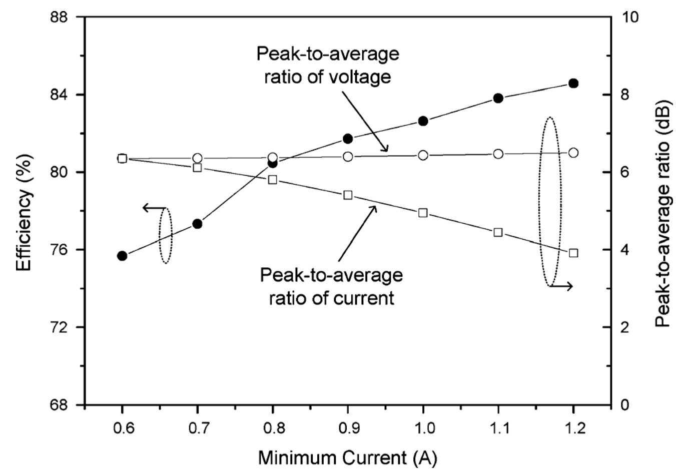

Fig. 7. PAR of current and voltage, efficiency of HSA versus minimum load current.

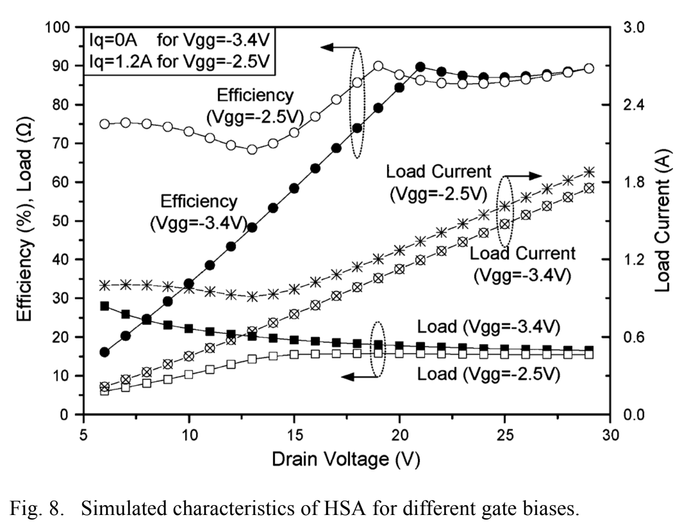

Fig. 8. Simulated characteristics of HSA for different gate biases.

of the HSA is depicted in Fig. 8. Even at a low and middle envelope region, most of the load current is generated by the switch and the efficiency is a lot higher than the conventional supply modulator. Therefore, the HSA achieves high efficiency for all of the power levels, and the average efficiency indicates over 80% for the modulated signal.

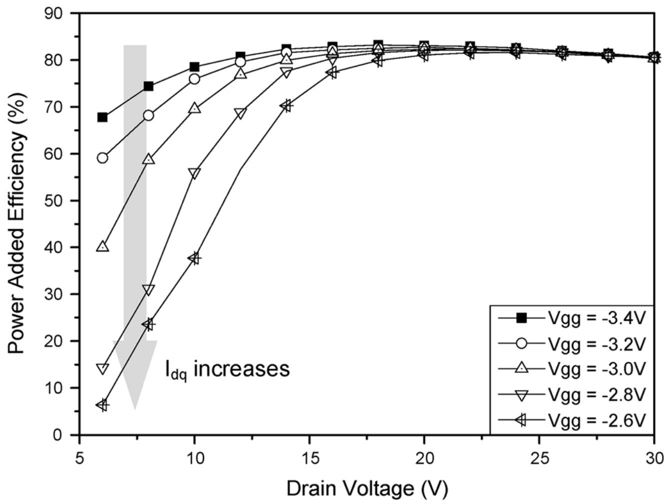

Fig. 9. Measured efficiency characteristics of PA for different gate biases.

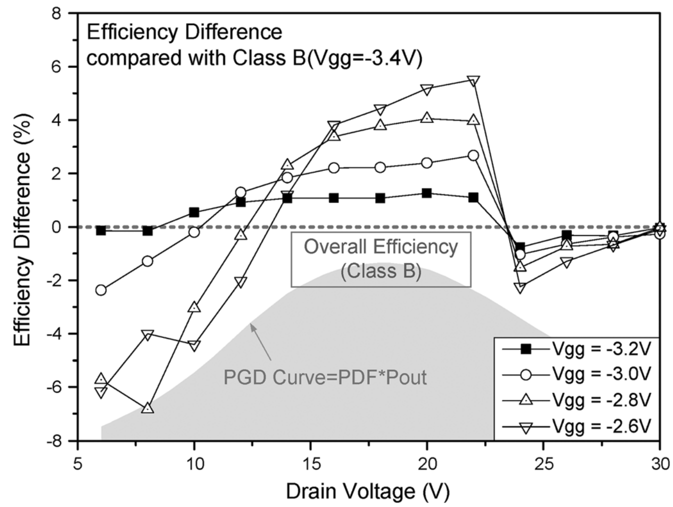

Fig. 10. Efficiency characteristics of ET PA for various gate biases (efficiency of PA: measured; efficiency of supply modulator: simulated).

In fact, when the quiescent current increases, the efficiency of the PA cannot help decreasing, as shown in Fig. 9. However, the reduction of the efficiency is very small at the high drain bias region because of the saturated mode operation. A saturated PA maintains high efficiency for the saturated operation with a large conduction angle, and a detailed explanation will be reported in the near future.

We can suppose that the required current of the PA is delivered from the wasted sinking current, and overall efficiency of the ET PA can be improved since the efficiency is multiplied by an efficiency of supply modulator and an efficiency of the PA shown as follows in (2):

$$\begin{aligned}\eta_{\rm ET}(V_{\rm ds}) &= \frac{P_{\rm out.PA}(V_{\rm ds})}{P_{\rm supply.SM}(V_{\rm ds})}\\ &= \frac{P_{\rm out.PA}(V_{\rm ds})}{P_{\rm supply.PA}(V_{\rm ds})}\cdot\frac{P_{\rm out.SM}(V_{\rm ds})}{P_{\rm supply.SM}(V_{\rm ds})}\\ &= \eta_{\rm PA}(V_{\rm ds})\cdot\eta_{\rm SM}(V_{\rm ds}). \qquad (2)\end{aligned}$$

Fig. 10 describes the efficiencies of the ET PA versus the gate bias voltages for various envelope voltage. The zero line indicates the efficiency of the class-B biased ET PA. In the low-power region, the efficiency reduction of the PA is much higher than the efficiency growth of the supply modulator, and in the high-power region, the efficiency of the supply modulator is also lower. Considering the efficiency distribution [12], however, we could expect that the high gate biased ET PA ($V_{\rm gs} = -2.6$ V) has higher efficiency than the class-B biased ET PA and the efficiency can be maximized by tracking the gate bias accordingly. In Section IV, we will verify that the overall efficiency of the ET PA is indeed increased for the high gate-biased PA.

III. RFIS for Optimum ET Operation

In Section II, we have focused on the voltage and current envelope shapings to increase the efficiency of the ET PA. In this section, we will concentrate on the RFIS to increase efficiency of the ET PA using the same signal. An ET PA usually uses an envelope signal for input signal of the supply modulator and a modulated RF signal for an input signal of the PA, respectively,

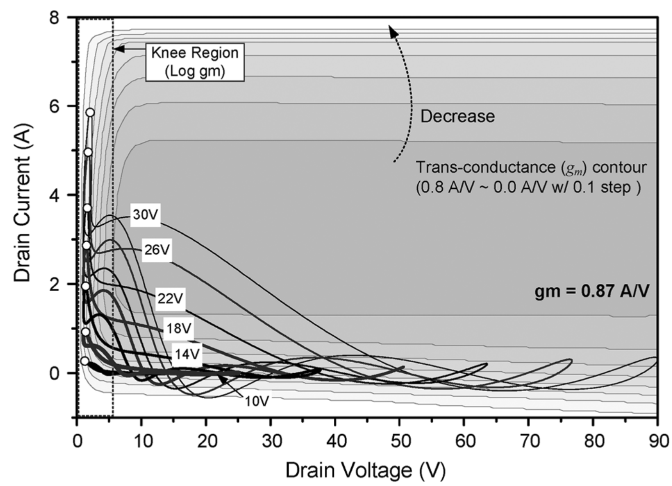

Fig. 11. Loadlines of ET PA and g_m variation.

which is called a hybrid envelope elimination and restoration (EER). Ideally, the PA operates in the saturated region for all of the power level because the envelope is proportional to the RF signal. However, in the practical case, the modulated RF signal does not guarantee uniformly saturated operation for all of the power level because of the nonlinear gain characteristic of the device. Fig. 11 shows g_m nonlinearity and loadlines of the PA for various drain biases. As shown on the *I–V* curve, g_m is not a constant, but has smaller value at lower V_{DD} and lower I_{DD}, and the PA does not operate at the properly saturated mode for any power levels, except for the peak power. Therefore, the PA cannot achieve maximum efficiencies for each V_{DD} value using the RF input signal. To solve this problem, the RF input power should be increased at a low power level to push into the high power-added efficiency (PAE) operation. Fig. 12 shows the maximum PAE point, before the gate turn-on, for various drain biases and the gains at the operation. From Fig. 12, we can find the optimum RFIS to achieve maximum PAE of the PA, and the conditions can be implemented using the simple shaping block. Fig. 13 describes the simple block diagram and the signal flows of the system. The envelope signal is linearly amplified by the

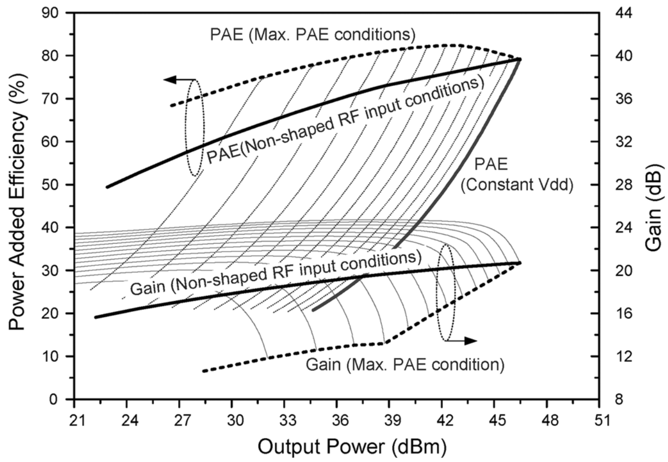

Fig. 12. Measured PAE and gain characteristics of the ET PA for various drain biases.

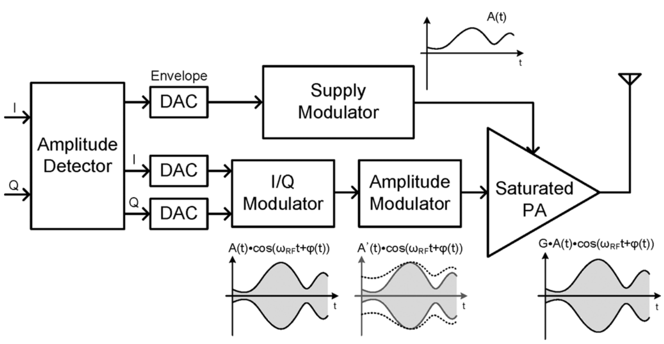

Fig. 13. Block diagram of RFIS system.

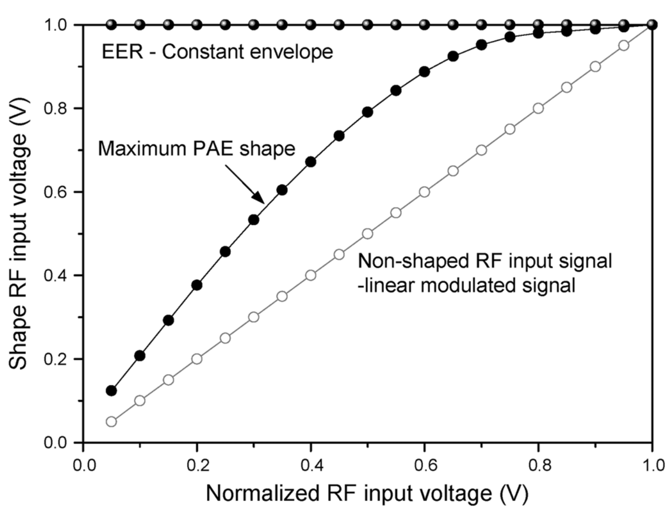

Fig. 14. Various RFIS.

supply modulator and the modulated RF signal is shaped by the amplitude modulator and is injected to the PA.

Fig. 14 describes several RF input shapes, constant envelope (EER), linear envelope and shaped envelope (maximum PAE). The shape for maximizing PAE has been found from the continuous wave (CW) measurement results, which can achieve maximum PAE of the PA. We will verify that the RFIS methods is valuable for the ET PA in Section IV.

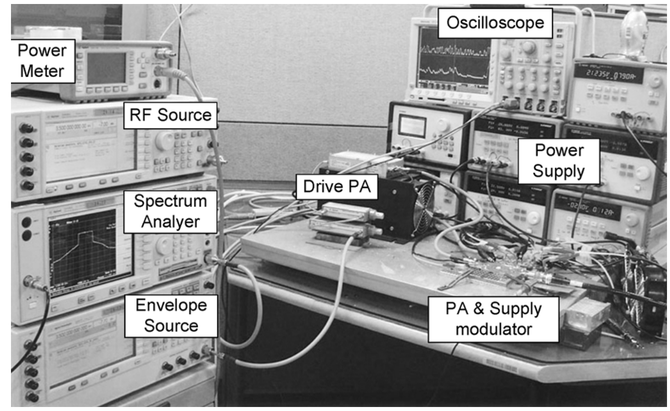

Fig. 15. Interlock experimental setup.

TABLE I
EXPERIMENTAL PERFORMANCES FOR THE DESIGNED ET PAs AT 889 MHz

	PAE[%]	DE[%]	Pout[dBm]	Gain[dB]
Conventional	53.18	54.16	39.57	17.46
USC	56.77	57.63	40.00	18.26
RFIS	58.76	60.21	40.14	16.19

IV. INTERLOCK EXPERIMENT RESULTS

In the previous sections, we have analyzed various efficiency enhancing methods of an ET PA, such as envelope voltage shaping, envelope current shaping, and RFIS. We have shown that the envelope voltage shaping is not effective, but the current shaping is to increase the efficiency of the supply modulator. In this case, efficiency of the supply modulator is increased due to the reduced sinking. The sinking current is redirected to the PA and utilized for amplification. The RFIS method adjusts the input power level for maximum PAE at each output level, and increases the ET PA efficiency. To verify these previous methods, an ET PA is implemented at 889 MHz, and is tested using the LTE signal with BW of 5 MHz and a PAPR of 6.5 dB. For the PA designs, a Cree CGH40045 GaN HEMT device is used to design a saturated PA [8]. The supply modulator is built using optimum discrete components for the best performance. Fig. 15 shows the interlock experimental setup. Two signal sources, the shaped RF signal and the envelope signal, are used for the supply modulator and the PA, respectively. For the ET PA, the delay between the PA and the supply modulator is the important factor because the performance is very sensitive to the delay. We have found the optimum delay adjusting ADS delay tab in the simulation and additional fine tuning coaxial cable line.

Table I shows performance summary of the methods. In the case of the conventional ET, the shaped envelope signal ($Vk = 6$ and $N = 1.4$) is used with the modulated input RF signal, and the gate bias of the PA is -3.2 V. As mentioned in Section II, the supplied envelope current is not determined by the envelope voltage shaping, but the input RF signal of the PA. Therefore, the envelope current is not shaped, and the minimum required current of the PA is very low for the deep class-AB bias case. Therefore, the sinking current of the supply modulator is wasted when the supply current is lower than the switch current. To

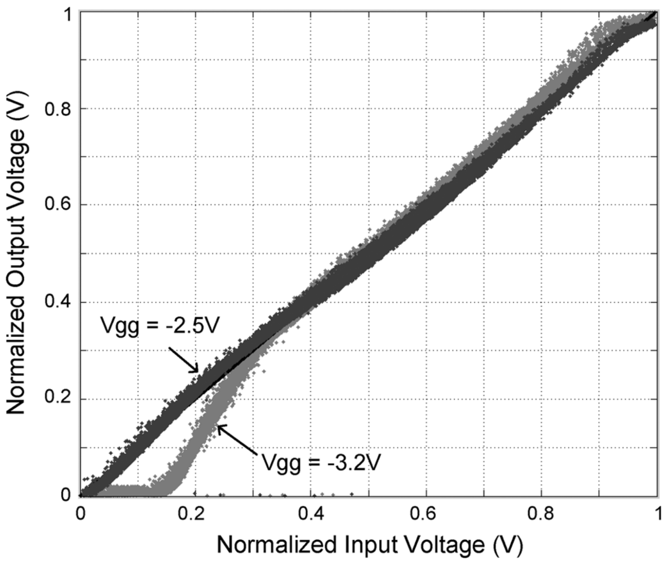

Fig. 16. AM–AM characteristic of ET PA for different gate biases.

TABLE II
EXPERIMENTAL PERFORMANCES FOR THE ET PA USING RFIS TECHNIQUE BEFORE AND AFTER DPDS AT 889 MHz

DPD	PAE[%]	DE[%]	Pout[dBm]	Gain[dB]
Before	58.76	60.21	40.14	16.19
After	58.35	59.72	40.00	16.42

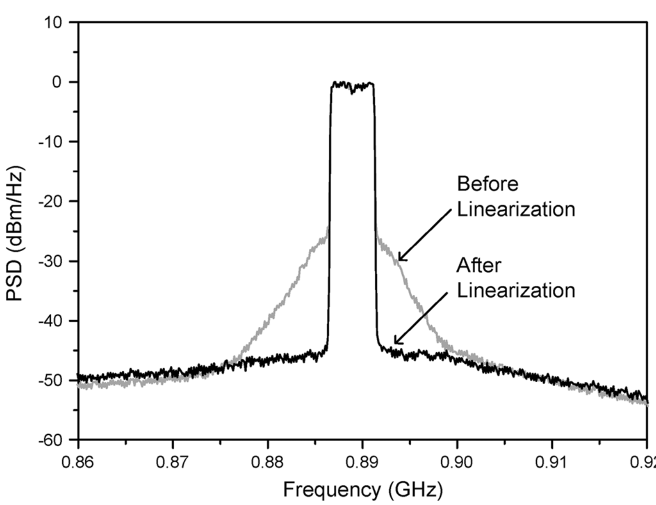

Fig. 17. Measured LTE spectra before and after the DPD linearization.

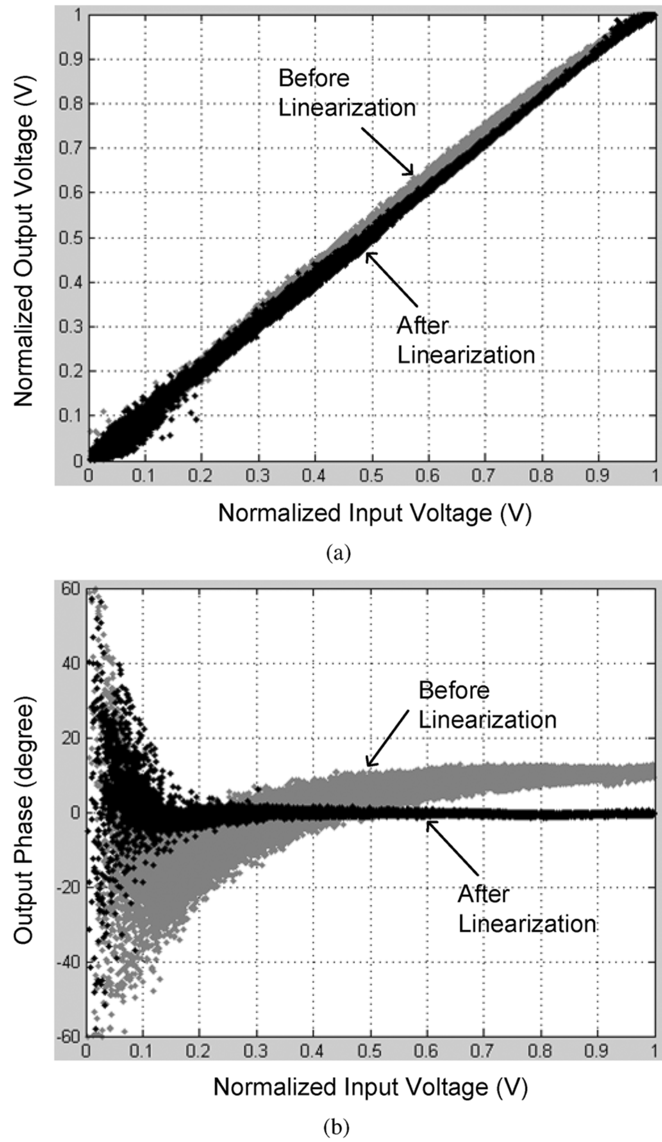

Fig. 18. (a) AM–AM characteristics before and after the DPD. (b) AM–PM characteristics before and after the DPD.

utilize the wasted current for amplification of the signal at the PA, the gate bias is increased from -3.2 to -2.5 V. The result is that PAE is improved by 3.59%, and gain and output power are also improved. Moreover, the linearity characteristic is improved significantly, as shown in Fig. 16. Usually, AM to AM response of the ET PA is severely bent at a low power region because of the low g_m. However, a higher gate bias for the USC enhances the g_m value, and the linear response of the AM–AM characteristic is obtained.

Additionally, the RFIS method is adapted for the interlock experiment. As a result, the PAE is improved by 2% additionally from the USC case. The proposed ET PA improved the PAE by 5.5% compared to the conventional case. The RFIS has a similar concept of the EER, thus this method is effective for a high-gain PA because the gain is compressed compared with the conventional ET PA.

For the linearization, we should pre-distort phase and magnitude information. However, the magnitude cannot be pre-distorted because the RFIS signal should be used to increase the efficiency, but the magnitude response can be compensated easily at the supply modulator since the RFIS method is based on the EER concept. The phase information is pre-distorted at the RFIS signal. Table II shows performances of the ET PA before and after linearization. This pre-distorted signal compensates the phase distortion and maintains the high efficiency of the PA. After linearization using the DPD techniques [22], [23], the ET PA can be linearized properly and delivers an output power of 40.00 dBm with a PAE of 58.35%. The ACLRs at 7.5- and 12.5-MHz offsets are improved below -45 dBc (Fig. 17), which satisfies the linearity specification of the LTE system. Fig. 18

shows the AM/AM and AM/PM characteristics of the PA before and after the linearization. The proposed ET PA does not show any gain reduction at a low power region because of the high quiescent current and it significantly reduces the high-order distortion.

V. CONCLUSION

We have proposed two methods of optimizing the ET PA. The first one is utilization of the sinking current to improved the performance of the supply modulator because the sinking current is a critical efficiency degradation factor. We increase the gate bias of the PA to deliver the sinking current to the PA and utilize it for amplification. This high current operation also improves the linearity of the PA. The other one is the RFIS, which increases the efficiency of the PA by operating at the maximum PAE for all power levels.

The implemented ET PA is tested for the LTE signal and delivers an output power of 40.14 dBm with a PAE of 58.76%, which is an improvement of the PAE by 5.5%. After applying linearization techniques of digital predistortion (DPD), adjacent channel leakage power ratio (ACLR) performances are within system specification, lower than -45 dBc. The proposed design methods are very useful to achieve a high-efficiency ET PA.

ACKNOWLEDGMENT

The authors would like to thank Cree Inc., Durham, NC, USA, for providing the large-signal model of the GaN HEMT used in this study.

REFERENCES

[1] F. H. Raab, P. Asbeck, S. Cripps, P. B. Kenington, Z. B. Popović, N. Pothecary, J. F. Sevic, and N. O. Sokal, "Power amplifiers and transmitters for RF and microwave," *IEEE Trans. Microw. Theory Techn.*, vol. 50, no. 3, pp. 814–826, Mar. 2002.

[2] J. Choi, D. Kang, D. Kim, J. Park, B. Jin, and B. Kim, "Power amplifiers and transmitters for next generation mobile handset," *J. Semicond. Technol. Sci.*, vol. 9, no. 4, pp. 249–256, Dec. 2009.

[3] P. B. Kenington*, High-Linearity RF Amplifier Design*. Norwood, MA, USA: Artech House, 2000.

[4] S. C. Cripps*, RF Power Amplifiers for Wireless Communications*. Norwood, MA, USA: Artech House, 2006.

[5] N. O. Sokal and A. D. Sokal, "Class-E: A new class of high-efficiency tuned single-ended switching power amplifiers," *IEEE J. Solid-State Circuits*, vol. SC-10, no. 6, pp. 168–176, Jun. 1975.

[6] F. H. Raab, "Class-F power amplifiers with maximally flat waveforms," *IEEE Trans. Microw. Theory Techn.*, vol. 45, no. 11, pp. 2007–2012, Nov. 1997.

[7] Y. Y. Woo, Y. Yang, and B. Kim, "Analysis and experiments for high-efficiency class-F and inverse class-F power amplifiers," *IEEE Trans. Microw. Theory Techn.*, vol. 54, no. 5, pp. 1969–1974, May 2006.

[8] J. Kim, J. Kim, J. Moon, J. Son, I. Kim, S. Jee, and B. Kim, "Saturated power amplifier optimized for efficiency using self-generated harmonic current and voltage," *IEEE Trans. Microw. Theory Techn.*, vol. 59, no. 8, pp. 2049–2058, Aug. 2011.

[9] F. H. Raab, "Efficiency of outphasing RF power-amplifier systems," *IEEE Trans. Commun.*, vol. COM-33, pp. 1094–1099, Oct. 1985.

[10] Y. Yang, J. Yi, Y. Y. Woo, and B. Kim, "Optimum design for linearity and efficiency of microwave Doherty amplifier using a new load matching technique," *Microw. J.*, vol. 44, no. 12, pp. 20–36, Dec. 2001.

[11] F. Wang, D. Kimball, J. Popp, A. Yang, D. Lie, P. Asbeck, and L. Larson, "An improved power-added efficiency 19-dBm hybrid envelope elimination and restoration power amplifier for 802.11g WLAN applications," *IEEE Trans. Microw. Theory Techn.*, vol. 54, no. 12, pp. 4086–4099, Dec. 2006.

[12] I. Kim, Y. Woo, J. Moon, J. Kim, J. Moon, J. Kim, and B. Kim, "High-efficiency hybrid EER transmitter using optimized power amplifier," *IEEE Trans. Microw. Theory Techn.*, vol. 56, no. 11, pp. 2582–2593, Nov. 2008.

[13] D. F. Kimball, J. Jeong, C. Hsia, P. Draxler, S. Lanfranco, W. Nagy, K. Linthicum, L. E. Larson, and P. M. Asbeck, "High-efficiency envelopetracking W-CDMA base-station amplifier using GaN HFETs," *IEEE Trans. Microw. Theory Techn.*, vol. 54, no. 11, pp. 3848–3856, Nov. 2006.

[14] J. Choi, D. Kim, D. Kang, and B. Kim, "A polar transmitter with CMOS programmable hysteretic-controlled hybrid switching supply modulator for multistandard applications," *IEEE Trans. Microw. Theory Techn.*, vol. 57, no. 7, pp. 1675–1686, Jul. 2009.

[15] G. B. Yundt, "Series- or parallel-connected composite amplifiers," *IEEE Trans. Power Elctron.*, vol. PE-1, no. 1, pp. 48–54, Jan. 1986.

[16] H. Ertl, J. W. Kolar, and F. C. Zach, "Basic considerations and topologies of switched-mode assisted linear power amplifiers," *IEEE Trans. Ind. Elctron.*, vol. 44, no. 1, pp. 116–123, Feb. 2007.

[17] D. Kim, D. Kang, J. Choi, J. Kim, Y. Cho, and B. Kim, "Optimization for envelope shaped operation of envelope tracking power amplifier," *IEEE Trans. Microw. Theory Techn.*, vol. 59, no. 7, pp. 1787–1795, Jul. 2011.

[18] J. Jeong, D. Kimball, M. Kwak, C. Hsia, P. Draxler, and P. Asbeck, "Wideband envelope tracking power amplifier with reduced bandwidth power supply waveform," in *IEEE MMT-S Int. Microw. Symp. Dig.*, Boston, MA, USA, Jun. 2009, pp. 1381–1384.

[19] C. Hsia, A. Zhu, J. Yan, P. Draxler, D. Kimball, S. Lanfranco, and P. Asbeck, "Digitally assisted dual-switch high-efficiency envelope amplifier for envelpe-tracking base-station power amplifiers," *IEEE Trans. Microw. Theory Techn.*, vol. 59, no. 11, pp. 2943–2952, Nov. 2011.

[20] A. Diet, C. Berland, M. Villegas, and G. Baudoin, "EER architecture specifications for OFDM transmitter using a class E amplifier," *IEEE Microw. Wireless Compon. Lett.*, vol. 14, no. 8, pp. 389–391, Aug. 2004.

[21] J. Kim, J. Moon, J. Son, S. Jee, J. Lee, J. Cha, I. Kim, and B. Kim, "Highly efficient envelope tracking transmitter by utilizing sinking current," in *Proc. 41th IEEE Eur. Microw. Conf.*, Manchester, U.K., Oct. 2011, pp. 636–639.

[22] Y. Y. Woo, J. Kim, J. Yi, S. Hong, I. Kim, J. Moon, and B. Kim, "Adaptive digital feedback predistortion technique for linearizing power amplifiers," *IEEE Trans. Microw. Theory Techn.*, vol. 55, no. 5, pp. 932–940, May 2007.

[23] J. Kim, Y. Y. Woo, J. Moon, and B. Kim, "A new wideband adaptive digital predistortion technique employing feedback linearization," *IEEE Trans. Microw. Theory Techn.*, vol. 56, no. 2, pp. 385–392, Feb. 2008.

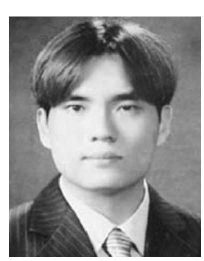

Jungjoon Kim (S'10) received the B.S. degree in electrical engineering from Han-Yang University, Ansan, Korea, in 2007, the Master degree in electrical engineering from the Pohang University of Science and Technology (POSTECH), Pohang, Gyungbuk, Korea, in 2009, and is currently working toward the Ph.D. degree at the POSTECH.

His current research interests include RF PA design and supply modulator design for highly efficient transmitter systems.

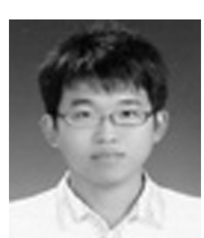

Junghwan Son (S'10) received the B.S. degree in physics from Sejong University, Seoul, Korea, in 2008, the M.S. degree in computer and communications engineering in from the Pohang University of Science and Technology (POSTECH), Gyeongbuk, Pohang, Korea, in 2010, and currently working toward the Ph.D. degree in electrical and electronics engineering at the POSTECH.

His current research interests include highly efficient Doherty PA design and DPD techniques.

Seunghoon Jee received the B.S. degree in electronic and electrical engineering from Kyungpook National University, Daegu, Korea, in 2009, and is currently working toward the Ph.D. degree at the Pohang University of Science and Technology (POSTECH), Gyeongbuk, Pohang, Korea.

His current research interests include highly linear and efficient RF PA design.

Seokhyeon Kim received the B.S. degree in electric engineering from the Pohang University of Science and Technology (POSTECH), Pohang, Gyungbuk, Korea, in 2011, and is currently working toward the Ph.D. degree at the POSTECH.

His current research interests include highly linear and efficient RF PA design.

Bumman Kim (M'78–SM'97–F'07) received the Ph.D. degree in electrical engineering from Carnegie Mellon University, Pittsburgh, PA, in 1979.

From 1978 to 1981, he was engaged in fiber-optic network component research with GTE Laboratories Inc. In 1981, he joined the Central Research Laboratories, Texas Instruments Incorporated, where he was involved in the development of GaAs power field-effect transistors (FETs) and monolithic microwave integrated circuits (MMICs). He has developed a large-signal model of a power FET, dual-gate FETs for gain control, high-power distributed amplifiers, and various millimeter-wave monolithic microwave integrated circuits (MMICs). In 1989, he joined the Pohang University of Science and Technology (POSTECH), Pohang, Gyungbuk, Korea, where he is currently a POSTECH Fellow and a Namko Professor with the Department of Electrical Engineering, and Director of the Microwave Application Research Center, where he is involved in device and circuit technology for RF integrated circuits (RFICs). He has authored over 300 technical papers.

Prof. Kim is a member of the Korean Academy of Science and Technology and the National Academy of Engineering of Korea. He was an associate editor for the IEEE TRANSACTIONS ON MICROWAVE THEORY AND TECHNIQUES. He was a Distinguished Lecturer of the IEEE Microwave Theory and Techniques Society (IEEE MTT-S) and an IEEE MTT-S Administrative Committee (AdCom) member.